Reciprocal hemizygosity analysis reveals that the Saccharomyces cerevisiae CGI121 gene affects lag time duration under enological conditions

Runze Li
University of Auckland
Rebecca C. Deed (rebecca.deed@auckland.ac.nz)
University of Auckland https://orcid.org/0000-0001-6121-6786

Research Article

Keywords: fermentation, lag time, quantitative trait loci, reciprocal hemizygosity analysis, wine, yeast

Posted Date: November 9th, 2020

DOI: https://doi.org/10.21203/rs.3.rs-46186/v2

Version of Record: A version of this preprint was published on March 3rd, 2021. See the published version at https://doi.org/10.1093/g3journal/jkab061.

Abstract

It is standard practice to ferment white wines at low temperatures (10-18ºC). However, low temperatures increase fermentation duration and risk of problem ferments, leading to significant costs. The lag duration at fermentation initiation is heavily impacted by temperature; therefore, identification of *Saccharomyces cerevisiae* genes impacting on fermentation kinetics is of interest for winemaking.

We selected 28 *S. cerevisiae* BY4743 single deletants, from a prior list of open reading frames (ORFs) mapped to quantitative trait loci (QTLs) on chromosomes VII and XIII, influencing the duration of fermentative lag time. Five BY4743 deletants, *Δapt1*, *Δcgi121*, *Δclb6*, *Δrps17a*, and *Δvma21*, differed significantly in their fermentative lag duration compared to BY4743 in synthetic grape medium (SGM) at 15ºC, over 72 h. Fermentation at 12.5ºC for 528 h confirmed the longer lag times of BY4743 *Δcgi121*, *Δrps17a*, and *Δvma21*. These three candidate ORFs were deleted in *S. cerevisiae* RM11-1a and S288C to perform single reciprocal hemizygosity analysis (RHA). RHA hybrids and single deletants of RM11-1a and S288C were fermented at 12.5ºC in SGM and lag time measurements confirmed that the S288C allele of *CGI121* on chromosome XIII, encoding a component of the EKC/KEOPS complex, increased fermentative lag phase duration. Nucleotide sequences of RM11-1a and S288C *CGI121* alleles differed by only one synonymous nucleotide, suggesting that codon bias or positional effects might be responsible for the impact on lag phase duration. This research demonstrates a new role of *CGI121* and highlights the applicability of QTL analysis for investigating complex phenotypic traits in yeast.

Introduction

Alcoholic fermentation for most white wines is performed at low temperatures (10-18°C), as this range generally results in greater production and retention of desirable volatiles, leading to high quality wines (García-Ríos et al. 2017; Molina et al. 2007; Llauradó et al. 2002). However, low temperatures also dramatically lengthen the time taken until fermentation completion and increase the risk of ferments becoming stuck or sluggish, which is potentially costly in terms of reduced winery space, product loss and decreased profits (Colombie et al. 2005; Llauradó et al. 2005; Beltran et al. 2007; López-Malo et al. 2013; Bisson 1999). Low temperatures encountered during fermentation are particularly stressful to yeast and cause changes in cell membrane fluidity, nutrient uptake and utilization, production of protective compounds, and a decrease in enzymatic reactions (Beltran et al. 2007; Ganucci et al. 2018; García-Ríos et al. 2016; Redón et al. 2011). A greater understanding of the genetics behind the ability of the wine yeast, *Saccharomyces cerevisiae*, to acclimate to low temperatures and perform fermentation more efficiently in general, is therefore useful for the wine industry.

The duration of the lag period at the start of fermentation, defined as the time between inoculation and the start of CO_2 release, and representing the time necessary for a yeast strain to acclimate to a new environment (Marullo et al. 2006), is greatly impacted by fermentation temperature, along with other variables encountered by yeast during fermentation. The high osmolarity of grape musts, along with the low pH, low oxygen availability, oxidative stress, and potentially high levels of sulfur dioxide (SO_2), low

levels of nutrients such as nitrogen, and to a lesser and strain-specific extent, phytosterols and thiamine, all contribute to the duration of the fermentative lag (Ferreira et al. 2017; Treu et al. 2014). Different *S. cerevisiae* strains also exhibit large variation in their fermentative lag duration ranging from a few hours up to a few days (Marullo et al. 2006; Camarasa et al. 2011). The genetic regulation controlling phenotypic variation in the fermentative lag time of different yeast strains is as complex as the variables involved and largely polygenic (Marullo et al. 2007; Marullo et al. 2006). During the first few hours after inoculation in enological conditions, yeast must respond to the new environment with a dramatic metabolic reorganization, resulting in an increase in the synthesis of transcripts and proteins involved in carbon and nitrogen metabolism, cellular stress response, ribosomal biogenesis, protein synthesis and oxidative stress (Salvadó et al. 2008; Rossignol et al. 2003). Within this response, there are likely to be numerous genes and QTLs that influence the duration of the lag phase before the release of CO_2. This response is more pronounced when the temperature of the must is low, lengthening the duration of the lag further (Salvadó et al. 2008; Albertin et al. 2017).

So far, one QTL with strong linkage to lag phase has been mapped to the *SSU1* gene, encoding the SO_2 efflux pump (Peltier et al. 2018). Removal of SO_2 from the yeast cell is carried out via Ssu1p, in which there are several allelic variants and translocation events in different strains that alter Ssu1p efficiency (Ferreira et al. 2017; Perez-Ortin et al. 2002). Beneficial genetic variants allow yeast to pump out SO_2 more efficiently, significantly reducing lag time. Previous work in our laboratory investigated QTLs linked to fermentation kinetics and found two regions, one of Chr. VII and one on Chr. XIII, that were significantly linked to fermentative lag (Deed et al. 2017). Linkage analysis was performed on a set of 119/121 completely mapped (> 99% of the genome) F_1 progeny from a cross between haploid strains BY4716 and RM11-1a constructed by Brem et al. (2002). Due to the difficulty in phenotyping lag phase in experiments with grape juice, and the large number of candidate genes within the confidence intervals surrounding the high LOD score peaks on Chr. VII (10 open reading frames ((ORFs) and Chr. VIII (34 ORFs), these 44 candidate genes were not investigated further. This previous identification of chromosomal regions linked to lag phase duration provides an excellent opportunity to investigate the causative genes using a controlled and reproducible fermentation medium, such as synthetic grape medium (SGM). Since single reciprocal hemizygosity analysis (RHA) was not feasible for 44 different genes, we first aimed to test the lag duration of BY4743 single deletants of each candidate ORF identified in Deed et al. (2017). Those demonstrating variation in lag time compared to the BY4743 reference strain would be deleted in haploids RM11-1a and S288C, followed by the construction of RHA hybrids. Phenotyping of deletants and RHA hybrids would confirm any relationships between the candidate ORFs with lag time phenotypes during fermentation.

Materials And Methods

S. cerevisiae strains

We utilized laboratory strain BY4743 (*MATa/α his3Δ1/his3Δ1 leu2Δ0/leu2Δ0 LYS2/lys2Δ0 met15Δ0/MET15 ura3Δ0/ura3Δ0*) and 28 BY4743 single deletants derived from EUROSCARF containing a Kanamycin resistance construct (*KanMX*) in place of each ORF of interest (Table 1). The deletants were selected based on an original list of 44 candidates linked to lag phase in Deed et al. (2017) after linkage analysis of 119/121 BY4716 × RM11-1a F_1 progeny using 2957 mapped loci (Brem et al. 2002). Of the 44 original candidates, 28 were available from EUROSCARF. Single gene deletions in three of the 28 candidates of interest were constructed in S288C (*MATα*), standing in for the BY4716 parent, and RM11-1a (*MATa HO::HphMX*) (Table 2). Combinations of wild type and deletant versions of S288C and RM11-1a were then used to make hybrids for RHA.

Growth and fermentation conditions

S. cerevisiae cultures were propagated using yeast peptone dextrose medium (YPD) medium and incubated overnight at 28°C, with orbital shaking at 150 revolutions per minute (rpm). BY4743 and BY4743 deletion mutants were fermented in 250-mL flasks with airlock at 12.5°C and 15°C in 100 mL SGM supplemented with additional amounts of the following amino acids: 10 × histidine (300 mg L^{-1}), 10 × leucine (300 mg L^{-1}) and 10 × uracil (100 mg L^{-1}) for auxotrophies (Harsch et al. 2010). RM11-1a and S288C wild types, deletants, and RHA hybrids were fermented at 12.5 °C in 13-mL tubes with 8 mL SGM. A < 0.5 mm^2 pin-hole was punctured into each tube lid to allow for CO_2 escape (Deed et al. 2017). All fermentations were inoculated at density of 1 × 10^6 cells mL^{-1} and were monitored either 8-hourly or daily by measuring cumulative weight loss (g) (Bely *et al.* 1990).

Analysis of kinetic parameters

The length of lag phase (h) of BY4743 and the 28 BY4743 deletants at 15°C was determined using the cumulative weight loss data to calculate the time elapsed between inoculation and the x-axis intercept where the steepest part of the slope transects y_0, as per Marullo *et al.* (2006). Lag phase duration for all fermentations performed at 12.5°C was measured using a Gompertz model with curve fitting based on Tronchoni et al. (2009) and executed using the R package nlstools (Baty et al. 2015).

Gene deletions and reciprocal hemizygosity analysis

Deletion of three candidate genes, *CGI121*, *RPS17a* and *VMA21*, within either the the Chr. VII or Chr. XIII QTLs linked to lag phase were constructed in RM11-1a Hgm^R and S288C using a modification of the Schiestl and Gietz (1989) lithium acetate yeast transformation protocol. Transformation of haploid RM11-1a and S288C was performed independently to generate mutants with *KanMX* insertions in *CGI121*, *RPS17a*, and *VMA21* by amplifying the corresponding constructs, *CGI121::KanMX*, *RPS17a::KanMX*, and *VMA21::KanMX*, from BY4743 EUROSCARF deletion library strains. Transformation with a Nat^R pFLR-A plasmid was used as a positive control. Successful deletions were confirmed via PCR (list of oligonucleotide primers in Table 3) and gel electrophoresis. Crosses were made between RM11-1a and S288C wild types, and combinations of non-deleted RM11-1a with each S288C deletion mutant and

vice versa, in order to construct diploid hemizygous F_1 hybrids for RHA (Steinmetz et al. 2002b) (crosses in Table 2). Since there were no markers in the S288C parent, this strain had to be present in 100 × excess of the RM11-1a deletion strain parent for mating (1×10^8 cells mL^{-1} S288C wild type with 1×10^6 cells mL^{-1} RM11-1a Hgm^R Kan^R deletion strain). Hybrids were selected on YPD plates containing 300 µg L^{-1} hygromycin B and 200 µg L^{-1} G-418. A multiplex PCR to amplify ten variable microsatellite markers and two mating type loci, *MATa* and *MATα*, was used to ensure that the hybridization was successful and to finalize strain selection since there would be some RM11-1a parents present when crossed with the marker-less S288C (Table 4) (Richards *et al.* 2009).

Statistical analysis and bioinformatics

All fermentation experiments were carried out in triplicate. Student's t-tests were carried out using Microsoft Excel with raw *p*-values reported, while ANOVA and post-hoc Tukey's HSD were performed using JASP software (version 0.12.2.0). Geneious Prime (version 2020.2.1) was used to align nucleotide sequences and translate to amino acids.

Results

First screening of 28 BY4743 deletion mutants fermented in SGM at 15°C identified five candidate ORFs that may influence lag time

Of the 44 *S. cerevisiae* genes identified within the 95% confidence intervals of the high LOD score peaks for QTLs on Chr. VII and Chr. XIII linked to fermentation lag duration in Deed et al. (2017), 28 single gene deletion mutants were available from EUROSCARF (listed in Table 1). Of the 16 ORFs that were unavailable, seven were classified as essential genes and hence inviable in a null mutant according to the Saccharomyces Genome Database. The remaining nine either encoded transposable elements (six ORFs) or were classified as dubious and unlikely to encode a protein (three ORFs). Cumulative weight loss (g) of the 28 BY4743 deletants fermented in 100 mL SGM at 15°C was measured at eight-hour intervals for 72 hours as a quick initial screen to identify whether any of the ORFs have an impact on the duration of the fermentative lag compared to the BY4743 reference (Figure 1A-D). Since it was not feasible to perform RHA on 28 different candidate genes, this initial step was conducted to narrow down the number of candidates. Due to the large number of fermentations in triplicate, the deletants were fermented in four separate batches, each with the BY4743 reference for standardization, and an uninoculated control as a measure of evaporation and to ensure there was no contamination.

Figure 1A-D shows that the 28 deletants demonstrated a range of fermentation abilities at 15ºC in SGM, with strong visual indications of variation in lag phase time compared to the BY4743 reference. The lag duration of BY4743 and the 28 deletants was calculated from the weight loss curves and presented in Figure 2A-D. The lag time for BY4743 across the four batches ranged from 40-52.8 h, with a mean of 45.7 h (n = 12). This degree of variation demonstrates the difficulty of measuring lag time due to the high level of noise at the start of fermentation. There were no significant differences between the BY4743 deletants

in batch 1 compared to BY4743 (Figure 2A). In batches 2 and 3, the lag phase times of BY4743 Δ*rps17a* (56.6 h) (Figure 2B) and BY4743 Δ*vma21* (48.7 h) (Figure 2C) were significantly longer than BY4743 (43.6 h), while BY4743 Δ*clb6* (37.3 h) had a significantly shorter lag phase (Figure 2C). In batch 4, two deletants, BY4743 Δ*apt1* and BY4743 Δ*cgi121*, had two replicates each that had not yet left lag phase (Figure 2D). For a useful comparison to be made against BY4743 (44.9 h), the lag times for these replicates were set at 70 h, giving an average duration of 63.5 h for BY4743 Δ*apt1* and 63.6 h for BY4743 Δ*cgi121*, although the actual measure of lag time is likely to be longer for these deletants.

Further screening at 12.5°C confirms that BY4743 single deletions of Δ*cgi121*, Δ*rps17a*, and Δ*vma1* significantly alter fermentative lag time

Since the five candidate genes identified above were selected across three different fermentation batches with a degree of noise, and with some strains still in fermentative lag or unable to ferment, a repeat single-batch 100-mL fermentation was performed for the five deletants and BY4743 to confirm that the lag phase differences observed were repeatable. The fermentations were also performed over a longer timeframe (528 h) than was used previously to determine whether the mutants that did not initiate fermentation were still in lag phase or were unable to ferment. A temperature of 12.5°C was selected to provide a greater resolution in lag phase duration compared to 15°C, whilst maintaining an enologically relevant temperature.

Figure 3 shows the weight loss curves at 12.5°C for the five deletants and BY4743. The results from the first screening at 15°C were conserved at 12.5°C, with BY4743 and BY4743 Δ*clb1* demonstrating an earlier exit from fermentative lag compared to BY4743 *Δcgi121*, BY4743 *Δrps17a*, and BY4743 Δ*vma21*. Surprisingly, with the extension of the fermentation timeframe, it was revealed that the performance of the Δ*apt1* deletant was equivalent to the uninoculated control, with no initiation of fermentation. The Δ*apt1* deletant was capable of growth in YPD in the fermentation precultures, suggesting that this strain may either be deficient in a specific factor required for fermentation and/or the enological environment was not permissible for the growth of this strain. The lag phase duration was calculated for the remaining strains using a modified Gompertz curve-fitting model to obtain greater accuracy compared to the intercept method used in the quick screen (Tronchoni et al. 2009). Overall, lag times at 12.5°C compared to 15°C were approximately two-fold longer, as expected when decreasing fermentation temperature (Charoenchai et al. 1998; Torija et al. 2003) (Figure 4). The lag times confirm the prior observations from the weight loss curves in Figure 3, but with no significant difference between the lag times of two fastest strains, BY4743 (64.9 h) and BY4743 Δ*clb1* (59.1 h) (Figure 4). The lag times of BY4743 Δ*cgi121* (149.6 h), BY4743 Δ*rps17a* (130.7 h), and BY4743 Δ*vma21* (119.9 h) were not significantly different from one another based on the 95% confidence intervals, but were significantly longer than the lag times of BY4743 and BY4743 Δ*clb6*.

To summarize, fermentation screening successfully identified three genes resulting in a longer lag phase when deleted (*Δcgi121*, *Δrps17a*, and Δ*vma21*). These were further investigated using single RHA.

Construction of RM11-1a and S288C single gene deletions and RHA hybrids reveals that the *CGI121* gene impacts on lag phase duration

To determine whether any of the three candidates, *CGI121* (Chr. XIII), *RPS17a* (Chr. XIII), or *VMA21*(Chr. VII), were responsible for the high LOD scores and genetic linkage to fermentative lag phase in the original 119 BY4716 × RM11-1a mapped progeny, single deletions of these three ORFs were constructed in two haploid *S. cerevisiae* strain backgrounds, RM11-1a (Hgm^R) and S288C. S288C was used as a substitute for BY4716, as in Deed et al. (2017). For the three candidate genes, all combinations of RM11-1a and S288C single deletants with the corresponding wild type were hybridized for RHA (Table 2). Successful hybridization was confirmed using microsatellite typing (Table 3).

Fermentation in SGM at 12.5°C was performed for 192 h, with 8-hourly monitoring, using the RM11-1a and S288C parent strains, the haploid Δ*cgi121*, Δ*rps17a*, and Δ*vma21* single deletants in RM11-1a and S288C, the RM11-1a × S288C F_1 hybrid and the RHA F_1 hybrids constructed by crossing combinations of RM11-1a and S288C. The RHA hybrids were hemizygous for a null allele and either the RM11-1a copy or the S288C copy of *CGI121*, *RPS17a*, or *VMA21*. Cumulative weight loss curves show that the diploid RM11-1a × S288C F_1 hybrid had a superior fermentation performance compared to the haploid parents, RM11-1a and S288C, based on the emergence from fermentative lag and rate of fermentation (Figure 5A-C). RM11-1a and S288C performed similarly, and in all cases exhibited a much shorter lag time compared to all RM11-1a and S288C single deletion mutants in Δ*cgi121*, Δ*rps17a*, and Δ*vma21*, in agreement with the results observed for BY4743. This result confirms that the presence of *CGI121*, *RPS17a* and *VMA1* results in faster lag times. The RM11-1a × S288C Δ*cgi121* hybrid appeared to exit fermentative lag at the same time as RM11-1a × S288C, while the lag phase of RM11-1a Δ*cgi121* × S288C was longer (Figure 5A). There did not appear to be any difference between RM11-1a × S288C Δ*rps17a* or RM11-1a Δ*rps17a* × S288C in terms of fermentation performance, and potentially only a minor difference in lag time compared to RM11-1a × S288C (Figure 5B). The same trend was observed for RM11-1a × S288C Δ*vma21* and RM11-1a Δ*vma21* × S288C; however, both hemizygotes showed a noticeably longer lag time than RM11-1a × S288C (Figure 5C).

Figure 6A confirms that the lag times for RM11-1a and S288C Δ*cgi121*, Δ*rps17a*, and Δ*vma21* single deletants were significantly longer than non-deleted RM11-1a and S288C (average of 390 h compared to 126 h), as suggested from the weight loss curves in Figure 5A-C. The long lag times of the deletion mutants corroborates the results shown by the BY4743 Δ*cgi121*, Δ*rps17a*, and Δ*vma21* deletants, but with even greater lag duration in RM11-1a and S288C due to the generally poor fermentation performance of haploid strains (Li et al. 2010). There were no significant differences between the non-deleted RM11-1a and S288C strains or between the corresponding pairs of RM11-1a and S288c single deletion mutants in Δ*cgi121*, Δ*rps17a*, or Δ*vma21*. Additionally, there were no significant differences in lag time between RM11-1a Δ*cgi121*, Δ*rps17a*, and Δ*vma21* single deletants. The same result was observed for the S288C single deletants. For the RHA hybrids (Figure 6B), the lag time of the RM11-1a × S288C Δ*cgi121* hybrid was not significantly different from the RM11-1a × S288C wild type (average of 122 h and 121 h, respectively). However, the RM11-1a Δ*cgi121* × S288C hybrid had a significantly longer

lag time (149 h), suggesting that the presence of the RM11-1a *CGI121* allele results in a lag time equivalent to wild type, but the S288C version results in increased lag time. This result is strong evidence validating the role of *CGI121* on impacting the duration fermentative lag and corresponds to mapping data indicating that the longer lag time is consistent with the presence of the S288C *CGI121* allele and not the RM11-1a copy in the homozygous F_1 progeny from the original cross (Deed et al. 2017). We aligned the RM11-1a and S288C nucleotide sequences of *CGI121* to determine whether there were any allelic differences. However, nucleotide alignment showed that the sequences were 99% identical and the single base difference observed at 282 bp (G in RM11-1a and A in S288C) was synonymous, with both codons corresponding to a phenylalanine (AAG vs. AAA) (Figure S1). Further alignment of 1 kb in front of the coding sequence of the RM11-1a and S288C *CGI121* sequences did not uncover any nucleotide differences in the promoter region.

For *RPS17a*, as suggested by the weight loss curves, there was no significant difference in lag time between RM11-1a × S288C Δ*rps17a* or RM11-1a Δ*rps17a* × S288C, suggesting that neither allele impacts on lag time, even though RM11-1a Δ*rps17a* × S288C did have a slightly longer lag than RM11-1a × S288C (138 h vs. 121 h). RM11-1a × S288C Δ*vma21* and RM11-1a Δ*vma21* × S288C were also not significantly different from one another, with no allele-specific impacts on lag duration for *VMA21*. The lag times for both hemizygotes were significantly longer than RM11-1a × S288C (144 and 149 h vs. 121 h) suggesting an additive effect with two copies of the *VMA21* gene being beneficial for a shorter lag time.

Overall, these results have demonstrated a clear role of *CGI121* on Chr. XIII for altering fermentative lag time, and although *RPS17a* and *VMA21* did not show allelic differences in terms of their impact on lag time, both genes have a clear affect on lag duration when deleted.

Discussion

Through genetic linkage analysis from a set of completely mapped 119 BY4716 × RM11-1a F_1 progeny, fermentation screening of single BY4743 deletants in candidate genes to narrow down the field, and RHA using RM11-1a and S288C, we have identified the relationship between the *CGI121* gene on Chr. XIII with fermentative lag time duration, which likely corresponds to the high LOD score on Chr. XIII (Deed et al. 2017). Deletion of Δ*cgi121* in homozygous diploid BY4743, and haploids RM11-1a and S288C, resulted in a significant increase in fermentative lag in SGM at 12.5°C, compared to the corresponding wild types. The effect of the *CGI121* gene in fermentative lag phase was different in the hemizygous single RHA F_1 hybrids, depending on whether they harboured the RM11-1a or the S288C allele, i.e. the RM11-1a Δ*cgi121* × S288C F_1 hybrid had a significantly longer fermentative lag duration than RM11-1a × S288C and RM11-1a × S288C Δ*cgi121*. Mapping data from Deed et al. (2017) determined that the difference in *CGI121* in the F_1 progeny was derived from the S288C allele. Transcriptomics data also demonstrated that *CGI121* transcripts are upregulated by at least 2-fold in an M2 × S288C F_1 hybrid vs. the M2 parent during the early stages of fermentation (at 2% weight loss) at 12.5°C, suggesting a key difference in the regulation

of the S288C *CGI121* allele. Although the single nucleotide difference between the RM11-1a and S288C *CGI121* alleles was synonymous, it has been reported that synonymous mutations can result in differences in gene expression, with the use of particular codons significantly increasing transcript numbers (Plotkin and Kudla 2011). Alternatively, there could be *cis* or *trans* regulatory effects depending on the allele position (Sinha et al. 2006; Brem et al. 2002).

Role of *CGI121* and evidence for impact on fermentative lag time

CGI121 (*YML036W*) is a 652 bp gene encoding a small polypeptide component of the *e*ndopeptidase-like and *k*inase associated to transcribed *c*hromatin (EKC)/*k*inase, *e*ndopeptidase and *o*ther *p*roteins of *s*mall size (KEOPS) protein complex (Srinivasan et al. 2011). The EKC/KEOPS complex is highly conserved and has roles in transcription, telomere uncapping, chromosome segregation, and DNA repair, and is specifically required for threonine carbamoyl adenosine (t^6A) tRNA modification and telomeric $TG_{1\text{-}3}$ recombination and length regulation (Srinivasan et al. 2011; Liu et al. 2018; Kisseleva-Romanova et al. 2006). There are five proteins within this complex, encoded by *BUD32*, *CGI121*, *GON7*, *KAE1*, and *PCC1*. Of the five genes, only Δ*kae1* null mutants are inviable, due to the severe growth impairment and chromosomal instability caused by deleting this essential gene, which encodes an ATPase (Mao et al. 2008; Downey et al. 2006). The role of Cgi121p in the EKC/KEOPS complex is to regulate Bud32p kinase activity by interacting with the N-terminal lobe, which in turn regulates the Kae1p ATPase, allowing for downstream function and catalytic activities (Mao et al. 2008; Zhang et al. 2015). Cgi121p does not directly participate in the t^6A tRNA modification function of the complex, but is important for telomere length regulation and recombination (Downey et al. 2006; Srinivasan et al. 2011; Peng et al. 2015), and may also be involved in creating stable connections between each KEOPS subunit, allowing for correct assembly (Perrochia et al. 2013). In *S. cerevisiae*, Cgi121p is the least essential of the five proteins in the EKC/KEOPS complex for retaining functionality but is required for maximal activity (Perrochia et al. 2013), with the phenotypes of Δ*cgi121* mutants being much milder than those displayed by Δ*kae1* or Δ*bud32* mutants (Mao et al. 2008; Kisseleva-Romanova et al. 2006; Downey et al. 2006).

Classical genetics studies have shown that null mutants of Δ*cgi121* have increased replicative lifespan and viability, and reduced single-stranded DNA at uncapped telomeres which functions to initiate telomere recombination (Downey et al. 2006; Peng et al. 2015). Deletion of Δ*cgi121* in BY4742 resulted in cells with a 50% longer lifespan, as the absence of *CGI121* inhibits telomere recombination and therefore provides greater genome stability (Peng et al. 2015). Large-scale surveys have implicated the Δ*cgi121* deletion in causing reduced vegetative and fermentative growth rates; however, data from Srinivasan et al. (Srinivasan et al. 2011) suggests that the vegetative growth of a W303-1A Δ*cgi121* mutant was close to wild type on solid medium after two days growth at 30°C. In the propagation of BY4743 Δ*cgi121* for fermentation in this research there did not appear to be any difference in vegetative growth in YPD compared to BY4743, with equivalent cell titres (data not shown), but there could be a difference in lag phase earlier on in vegetative growth which was not observable after 24 hours of growth at 28°C. In terms of fermentative growth, Δ*cgi121* was identified by Steinmetz et al. (2002a) as showing reduced growth on YPD with 2% glucose; however, this screen was aerobic and does not adequately represent the

fermentation environment. Hoose et al. (2012) identified S288C mutants in Δ*cgi121* as having an increased duration of cell cycle progression in G_1 phase, with the percentage of S288C Δ*cgi121* G_1 cells greater than two standard deviations (41.6%) above wild type S288C at equivalent measurement times. The longer period spent in G_1 phase would mean that Δ*cgi121* cells do not divide as often as wild type and can explain the longer lag time during fermentation. Cell division and vegetative growth influences the timeframe of the fermentative lag phase and stressful environmental conditions, such as those encountered in the enological environment can significantly prolong G_1 (Hoose et al. 2012), which could be why the impact of the Δ*cgi121* was more pronounced during fermentation at low temperature. The presence of certain nutrients also influences the timing through G_1 to START, from where the rest of the growth cycle can be completed. When shifting from poor to rich medium, the G_1 phase can be prolonged temporarily until the cells reach a critical size allowing them to commit to a phase of cell division (Hoose et al. 2012). In Δ*cgi121* mutants, there is a decreased rate of carbon and nitrogen utilization, with abnormal glucose and arginine metabolism (VanderSluis et al. 2014), as well as an upregulation of carbohydrate metabolism genes in Δ*cgi121* mutants compared to wild type (Chou et al. 2017). Therefore, abnormal usage of glucose, a primary carbon source in grape juice and SGM, as well as decreased nitrogen consumption and accumulation of arginine, could greatly impact on the lag duration of Δ*cgi121* mutants during fermentation.

Impact of *RPS17a* and *VMA21* on fermentative lag duration

We have also shown that along with the single deletion in Δ*cgi121*, single deletions in Δ*rps17a* (encoding a ribosomal protein of the small 40S subunit (Abovich et al. 1985)), and Δ*vma21* (encoding an integral membrane protein required for V-ATPase function (Hill and Stevens 1994)) resulted in an extended lag time duration in BY4743, RM11-1a and S288C; however, neither *RPS17a* nor *VMA21* provided clear evidence for any allelic differences via RHA analysis. Interestingly, Δ*rps17a* mutants demonstrate a prolonged G_1 phase in the cell cycle, in the same way as Δ*cgi121* (Hoose et al. 2012), which could explain the influence of the null mutant on fermentative lag. Null mutations in Δ*vma21*, result in a multitude of phenotypes in *S. cerevisiae*, with decreased resistance to oxidative and osmotic stress (Dudley et al. 2005), and decreased thermotolerance (Jarolim et al. 2013), all of which can result in a longer fermentative lag time (Ferreira et al. 2017). Although Δ*vma21* mutants also had a decreased carbon utilization rate, these were for non-fermentable carbon sources (VanderSluis et al. 2014; Dudley et al. 2005). The QTL responsible for the high LOD score on Chr. VII in Deed et al. (2017) is yet to be identified, but may be derived from the RM11-1a parent, which would mean that the initial BY4743 screen was not so useful for pinpointing the QTL responsible.

Conclusions

We have shown that single deletions of Δ*cgi121*, Δ*rps17a* and Δ*vma21* result in increased fermentative lag duration in *S. cerevisiae*. This research has also demonstrated that the *CGI121* gene, encoding a component of the EKC/KEOPS complex, plays a role in modulating the fermentative lag phase in *S.*

cerevisiae. Allele swaps via RHA confirmed that the S288C-derived *CGI121* allele accounted for a longer lag time. A greater understanding of the role of the *CGI121* in stress tolerance will allow easier manipulation and/or selection of *S. cerevisiae* strains to shorten or lengthen lag time and provide growth advantages during the fermentation of foods and beverages.

Declarations

Acknowledgments

The authors would like to thank Kristine Boxen (Genomics Unit, School of Biological Sciences, University of Auckland) for processing the microsatellite samples and Chien-Wei (Max) Huang for assisting RL in the laboratory.

Data availability

All data pertaining to this manuscript has been supplied. File S1 contains an alignment of RM11-1a and S288C *CGI121* nucleotide sequences.

Funding

This work was supported by internal funding from the School of Chemical Sciences, University of Auckland.

Conflicts of Interest

The authors declare that they have no conflicts of interest.

References

Abovich, N., L. Gritz, L. Tung, and M. Rosbash, 1985 Effect of *RP51* gene dosage alterations on ribosome synthesis in *Saccharomyces cerevisiae*. *Molecular and Cellular Biology* 5 (12):3429-3435.

Albertin, W., A. Zimmer, C. Miot-Sertier, M. Bernard, J. Coulon *et al.*, 2017 Combined effect of the *Saccharomyces cerevisiae* lag phase and the non-*Saccharomyces* consortium to enhance wine fruitiness and complexity. *Applied Microbiology and Biotechnology* 101 (20):7603-7620.

Baty, F., C. Ritz, S. Charles, M. Brutsche, J. Flandrois *et al.*, 2015 A Toolbox for Nonlinear Regression in R: The Package nlstools. *Journal of Statistical Software* 66 (5):1-21.

Beltran, G., N. Rozes, A. Mas, and J.M. Guillamon, 2007 Effect of low-temperature fermentation on yeast nitrogen metabolism. *World Journal of Microbiology and Biotechnology* 23 (6):809-815.

Bisson, L.F., 1999 Stuck and sluggish fermentations. *American Journal of Enology and Viticulture* 50 (1):107-119.

Brem, R.B., G. Yvert, R. Clinton, and L. Kruglyak, 2002 Genetic dissection of transcriptional regulation in budding yeast. *Science* 296 (5568):752-755.

Camarasa, C., I. Sanchez, P. Brial, F. Bigey, and S. Dequin, 2011 Phenotypic landscape of *Saccharomyces cerevisiae* during wine fermentation: Evidence for origin-dependent metabolic traits. *PloS One* 6 (9).

Charoenchai, C., G.H. Fleet, and P.A. Henschke, 1998 Effects of temperature, pH, and sugar concentration on the growth rates and cell biomass of wine yeasts. *American Journal of Enology and Viticulture* 49 (3):283-288.

Chou, H.J., E. Donnard, H.T. Gustafsson, M. Garber, and O.J. Rando, 2017 Transcriptome-wide Analysis of Roles for tRNA Modifications in Translational Regulation. *Molecular Cell* 68 (5):978-992.e974.

Colombie, S., S. Malherbe, and J.M. Sablayrolles, 2005 Modeling alcoholic fermentation in enological conditions: feasibility and interest. *American Journal of Enology and Viticulture* 56 (3):238-245.

Deed, R.C., B. Fedrizzi, and R.C. Gardner, 2017 *Saccharomyces cerevisiae FLO1* gene demonstrates genetic linkage to increased fermentation rate at low temperatures. *G3: Genes, Genomes, Genetics* 7 (3):1039-1048.

Downey, M., R. Houlsworth, L. Maringele, A. Rollie, M. Brehme *et al.*, 2006 A Genome-Wide Screen Identifies the Evolutionarily Conserved KEOPS Complex as a Telomere Regulator. *Cell* 124 (6):1155-1168.

Dudley, A.M., D.M. Janse, A. Tanay, R. Shamir, and G.M. Church, 2005 A global view of pleiotropy and phenotypically derived gene function in yeast. *Molecular Systems Biology* 1.

Ferreira, D., V. Galeote, I. Sanchez, J.L. Legras, A. Ortiz-Julien *et al.*, 2017 Yeast multistress resistance and lag-phase characterisation during wine fermentation. *FEMS Yeast Research* 17 (6).

Ganucci, D., S. Guerrini, S. Mangani, M. Vincenzini, and L. Granchi, 2018 Quantifying the effects of ethanol and temperature on the fitness advantage of predominant *Saccharomyces cerevisiae* strains occurring in spontaneous wine fermentations. *Frontiers in Microbiology* 9 (JUL).

García-Ríos, E., M. Morard, L. Parts, G. Liti, and J.M. Guillamón, 2017 The genetic architecture of low-temperature adaptation in the wine yeast *Saccharomyces cerevisiae*. *BMC Genomics* 18 (1).

García-Ríos, E., L. Ramos-Alonso, and J.M. Guillamón, 2016 Correlation between low temperature adaptation and oxidative stress in *Saccharomyces cerevisiae*. *Frontiers in Microbiology* 7 (AUG).

Harsch, M.J., S.A. Lee, M.R. Goddard, and R.C. Gardner, 2010 Optimized fermentation of grape juice by laboratory strains of *Saccharomyces cerevisiae*. *FEMS Yeast Research* 10 (1):72-82.

Hill, K.J., and T.H. Stevens, 1994 Vma21p is a yeast membrane protein retained in the endoplasmic reticulum by a di-lysine motif and is required for the assembly of the vacuolar H+-ATPase complex.

Molecular Biology of the Cell 5 (9):1039-1050.

Hoose, S.A., J.A. Rawlings, M.M. Kelly, C. Leitch, Q.O. Ababneh *et al.*, 2012 A systematic analysis of cell cycle regulators in yeast reveals that most factors act independently of cell size to control initiation of division. *PLoS Genetics* 8 (3).

Jarolim, S., A. Ayer, B. Pillay, A.C. Gee, A. Phrakaysone *et al.*, 2013 *Saccharomyces cerevisiae* genes involved in survival of heat shock. *G3: Genes, Genomes, Genetics* 3 (12):2321-2333.

Kisseleva-Romanova, E., R. Lopreiato, A. Baudin-Baillieu, J.C. Rousselle, L. Ilan *et al.*, 2006 Yeast homolog of a cancer-testis antigen defines a new transcription complex. *EMBO Journal* 25 (15):3576-3585.

Li, B.Z., J.S. Cheng, M.Z. Ding, and Y.J. Yuan, 2010 Transcriptome analysis of differential responses of diploid and haploid yeast to ethanol stress. *Journal of Biotechnology* 148 (4):194-203.

Liu, Y.Y., M.H. He, J.C. Liu, Y.S. Lu, J. Peng *et al.*, 2018 Yeast KEOPS complex regulates telomere length independently of its t6A modification function. *Journal of Genetics and Genomics* 45 (5):247-257.

Llauradó, J.M., N. Rozès, R. Bobet, A. Mas, and M. Constantí, 2002 Low temperature alcoholic fermentations in high sugar concentration grape musts. *Journal of Food Science* 67 (1):268-273.

Llauradó, J.M., N. Rozès, M. Constanti, and A. Mas, 2005 Study of some *Saccharomyces cerevisiae* strains for winemaking after preadaptation at low temperatures. *Journal of Agricultural and Food Chemistry* 53 (4):1003-1011.

López-Malo, M., A. Querol, and J.M. Guillamon, 2013 Metabolomic comparison of *Saccharomyces cerevisiae* and the cryotolerant species *S. bayanus* var. *uvarum* and *S. kudriavzevii* during wine fermentation at low temperature. *PloS One* 8 (3):1-14.

Mao, D.Y.L., D. Neculai, M. Downey, S. Orlicky, Y.Z. Haffani *et al.*, 2008 Atomic Structure of the KEOPS Complex: An Ancient Protein Kinase-Containing Molecular Machine. *Molecular Cell* 32 (2):259-275.

Marullo, P., M. Aigle, M. Bely, I. Masneuf-Pomarède, P. Durrens *et al.*, 2007 Single QTL mapping and nucleotide-level resolution of a physiologic trait in wine *Saccharomyces cerevisiae* strains. *FEMS Yeast Research* 7 (6):941-952.

Marullo, P., M. Bely, I. Masneuf-Pomarède, M. Pons, M. Aigle *et al.*, 2006 Breeding strategies for combining fermentative qualities and reducing off-flavor production in a wine yeast model. *FEMS Yeast Research* 6 (2):268-279.

Molina, A.M., J.H. Swiegers, C. Varela, I.S. Pretorius, and E. Agosin, 2007 Influence of wine fermentation temperature on the synthesis of yeast-derived volatile aroma compounds. *Applied Microbiology and Biotechnology* 77 (3):675-687.

Peltier, E., V. Sharma, M. Martí Raga, M. Roncoroni, M. Bernard *et al.*, 2018 Dissection of the molecular bases of genotype x environment interactions: A study of phenotypic plasticity of *Saccharomyces cerevisiae* in grape juices. *BMC Genomics* 19 (1).

Peng, J., M.H. He, Y.M. Duan, Y.T. Liu, and J.Q. Zhou, 2015 Inhibition of Telomere Recombination by Inactivation of KEOPS Subunit Cgi121 Promotes Cell Longevity. *PLoS Genetics* 11 (3).

Perez-Ortin, J.E., A. Querol, S. Puig, and E. Barrio, 2002 Molecular characterization of a chromosomal rearrangement involved in the adaptive evolution of yeast strains. *Genome Research* 12 (10):1533-1539.

Perrochia, L., D. Guetta, A. Hecker, P. Forterre, and T. Basta, 2013 Functional assignment of KEOPS/EKC complex subunits in the biosynthesis of the universal t6A tRNA modification. *Nucleic Acids Research* 41 (20):9484-9499.

Plotkin, J.B., and G. Kudla, 2011 Synonymous but not the same: The causes and consequences of codon bias. *Nature Reviews Genetics* 12 (1):32-42.

Redón, M., J.M. Guillamón, A. Mas, and N. Rozès, 2011 Effect of growth temperature on yeast lipid composition and alcoholic fermentation at low temperature. *European Food Research and Technology* 232 (3):517-527.

Rossignol, T., L. Dulau, A. Julien, and B. Blondin, 2003 Genome-wide monitoring of wine yeast gene expression during alcoholic fermentation. *Yeast* 20 (16):1369-1385.

Salvadó, Z., R. Chiva, S. Rodriguez-Vargas, F. Randez-Gil, A. Mas *et al.*, 2008 Proteomic evolution of a wine yeast during the first hours of fermentation. *FEMS Yeast Research* 8 (7):1137-1146.

Sinha, H., B.P. Nicholson, L.M. Steinmetz, and J.H. McCusker, 2006 Complex genetic interactions in a quantitative trait locus. *PLoS Genetics* 2 (2):140-147.

Srinivasan, M., P. Mehta, Y. Yu, E. Prugar, E.V. Koonin *et al.*, 2011 The highly conserved KEOPS/EKC complex is essential for a universal tRNA modification, t6A. *EMBO Journal* 30 (5):873-881.

Steinmetz, L.M., C. Scharfe, A.M. Deutschbauer, D. Mokranjac, Z.S. Herman *et al.*, 2002a Systematic screen for human disease genes in yeast. *Nature Genetics* 31 (4):400-404.

Steinmetz, L.M., H. Sinha, D.R. Richards, J.I. Spiegelman, P.J. Oefner *et al.*, 2002b Dissecting the architecture of a quantitative trait locus in yeast. *Nature* 416 (6878):326-330.

Torija, M.J., N. Rozes, M. Poblet, J.M. Guillamon, and A. Mas, 2003 Effects of fermentation temperature on the strain population of *Saccharomyces cerevisiae*. *International Journal of Food Microbiology* 80 (1):47-53.

Treu, L., S. Campanaro, C. Nadai, C. Toniolo, T. Nardi *et al.*, 2014 Oxidative stress response and nitrogen utilization are strongly variable in *Saccharomyces cerevisiae* wine strains with different fermentation performances. *Applied Microbiology and Biotechnology* 98 (9):4119-4135.

Tronchoni, J., A. Gamero, F.N. Arroyo-López, E. Barrio, and A. Querol, 2009 Differences in the glucose and fructose consumption profiles in diverse *Saccharomyces* wine species and their hybrids during grape juice fermentation. *International Journal of Food Microbiology* 134 (3):237-243.

VanderSluis, B., D.C. Hess, C. Pesyna, E.W. Krumholz, T. Syed *et al.*, 2014 Broad metabolic sensitivity profiling of a prototrophic yeast deletion collection. *Genome Biology* 15 (4).

Zhang, W., B. Collinet, M. Graille, M.C. Daugeron, N. Lazar *et al.*, 2015 Crystal structures of the Gon7/Pcc1 and Bud32/Cgi121 complexes provide a model for the complete yeast KEOPS complex. *Nucleic Acids Research* 43 (6):3358-3372.

Tables

Table 1 List of 28 ORFs identified within one LOD unit either side of the LOD >3 peak markers influencing lag phase duration in the *S. cerevisiae* genome and available as single deletions in BY4743 from EUROSCARF. Descriptions of protein function were obtained from the *Saccharomyces* Genome Database.

Chromosome	LOD score	ORF	Gene	Function
VII	2.235-2.570	*YGR104C*	*SRB5*	Subunit of the RNA polymerase II mediator complex
VII	2.642-3.000	*YGR105W*	*VMA21*	Integral membrane protein required for V-ATPase function
VII	2.642-3.000	*YGR106C*	*VOA1*	ER protein that functions in assembly of the V0 sector of V-ATPase
VII	2.642-3.000	*YGR107W*	*NA*	Dubious open reading frame
VII	2.642-3.000	*YGR108W*	*CLB1*	B-type cyclin involved in cell cycle progression
VII	2.978	*YGR109C*	*CLB6*	B-type cyclin involved in DNA replication during S phase
VII	2.979-2.030	*YGR110W*	*CLD1*	Mitochondrial cardiolipin-specific phospholipase
XIII	2.606	*YML048W*	*GSF2*	Endoplasmic reticulum localized integral membrane protein
XIII	2.606-3.175	*YML047C*	*PRM6*	Potassium transporter that mediates K^+ influx
XIII	2.606-3.175	*YML042W*	*CAT2*	Carnitine acetyl-CoA transferase
XIII	2.606-3.175	*YML041C*	*VPS71*	Nucleosome-binding component of the SWR1 complex
XIII	3.175	*YML038C*	*YMD8*	Putative nucleotide sugar transporter
XIII	3.119-2.720	*YML037C*	*NA*	Putative protein of unknown function
XIII	2.478	*YML036W*	*CGI121*	Component of the EKC/KEOPS complex
XIII	2.547-3.681	*YML035C*	*AMD1*	AMP deaminase
XIII	2.547-3.681	*YML034W*	*SRC1*	Inner nuclear membrane protein
XIII	2.547-3.681	*YML032C*	*RAD52*	Protein that stimulates strand exchange
XIII	3.725-3.373	*YML030W*	*RCF1*	Cytochrome c oxidase subunit
XIII	3.725-3.373	*YML029W*	*USA1*	Scaffold subunit of the Hrd1p ubiquitin ligase
XIII	3.725-3.373	*YML028W*	*TSA1*	Thioredoxin peroxidase
XIII	3.725-3.373	*YML027W*	*YOX1*	Homeobox transcriptional repressor; binds to Mcm1p and early cell cycle boxes in promoters of cell cycle genes
XIII	3.725-3.373	*YML026C*	*RPS18B*	Protein component of the small (40S) ribosomal subunit
XIII	3.725-3.373	*YML024W*	*RPS17A*	Ribosomal protein 51 (rp51) of the small (40s) subunit
XIII	3.328	*YML022W*	*APT1*	Adenine phosphoribosyltransferase
XIII	3.421-3.288	*YML021C*	*UNG1*	Uracil-DNA glycosylase
XIII	3.421-3.288	*YML020W*	*NA*	Protein of unknown function
XIII	3.421-3.288	*YML019W*	*OST6*	Subunit of the oligosaccharyltransferase complex of the ER lumen

XIII	3.288	*YML018C*	*NA*	Protein of unknown function

Table 2 List of RM11-1a and S288C RHA crosses to investigate the impact of the *CGI121*, *RPS17a* and *VMA1* loci. The genotypes are given for each of the RM11-1a and S288C parents. The S288C parent strain in bold was required to be present in 100 × excess of the RM11-1a parent, due to the lack of selectable markers to differentiate it from RM11-1a. The F_1 hybrid selections marked with * could result in the presence of the RM11-1a parent and the F_1 hybrid. The RM11-1a x S288c cross was included as a control.

Cross	Parent #1	Parent #2	F_1 hybrid selection
RM11-1a x S288C	RM11-1a (*HO::HphMX; MATa*)	**S288C (*MATα*)**	*HGM^R
RM11-1a x S288C Δ*cgi121*	RM11-1a (*HO::HphMX; MATa*)	S288C (*CGI121::KanMX; MATα*)	HGM^R; Kan^R
RM11-1a x S288C Δ*rps17a*	RM11-1a (*HO::HphMX; MATa*)	S288C (*RPS17a::KanMX; MATα*)	HGM^R; Kan^R
RM11-1a x S288C Δ*vma21*	RM11-1a (*HO::HphMX; MATa*)	S288C (*VMA21::KanMX; MATα*)	HGM^R; Kan^R
RM11-1a Δ*cgi121* x S288C	RM11-1a (*HO::HphMX; CGI121::KanMX; MATa*)	**S288C (*MATα*)**	*HGM^R; Kan^R
RM11-1a Δ*rps17a* x S288C	RM11-1a (*HO::HphMX; RPS17a::KanMX; MATa*)	**S288C (*MATα*)**	*HGM^R; Kan^R
RM11-1a Δ*vma21* x S288C	RM11-1a (*HO::HphMX; VMA21::KanMX; MATa*)	**S288C (*MATα*)**	*HGM^R; Kan^R

Table 3 Oligonucleotide primers used for gene deletions and RHA.

Primer name	Sequence (5' to 3')	Purpose
3'kanI-F	GGTCGCTATACTGCTGTC	Confirm integration of *KanMX* constructs
*CGI121*intL-F	CGGAATTAGCCCACGTAGAA	Amplification of *KanMX* from BY4743 Δ*cgi121* deletant
*CGI121*intR-R	GGAGAACTTTTGGCAGTTCG	Amplification of *KanMX* from BY4743 Δ*cgi121* deletant
*CGI121*testR-R	TATCGCAATGTCACCCCTTT	Flanking test primer to confirm integration of *KanMX* in the *CGI121* locus of transformants
*RPS17a*intL-F	GGCAGTGGTAGCTTGGTAGC	Amplification of *KanMX* from BY4743 Δ*rps17a* deletant
*RPS17a*intR-R	CAGATGGCGTTTCATTTTG	Amplification of *KanMX* from BY4743 Δ*rps17a* deletant
*RPS17a*testR-R	GGAGGAAACTGATTGGGTCA	Flanking test primer to confirm integration of *KanMX* in the *RPS17a* locus of transformants
*VMA21a*intL-F	AGGAACCCTCCGCTTGTTAT	Amplification of *KanMX* from BY4743 Δ*vma21* deletant
*VMA21*intR-R	GGTTGGGCTTTTGAAGATGA	Amplification of *KanMX* from BY4743 Δ*vma21* deletant
*VMA21*testR-R	TTCCAAAACTGTGCAAGCAG	Flanking test primer to confirm integration of *KanMX* in the *VMA21* locus of transformants

Table 4 Microsatellite confirmation of F_1 hybrid strains between RM11-1a and S288C for RHA. Numbers are band sizes in bp. The 12 loci detected correspond to 10 variable microsatellite loci and two mating type loci, *MATa* and *MATα*, as described in Richards *et al.* (2009).

Strain	*C3*	*C5*	*C8*	*C4*	*091c*	*AT4*	*AT2*	*Scaat3*	*009c*	*267c*	*α*	*a*
RM11-1a	121	139	146	259	260	296	364	381	419	-	-	480
S288C	120	174	130	240	303	296	358	407	443	-	457	-
RM11-1a x S288C	120, 121	139, 174	130, 146	240, 259	260, 303	296	358, 364	381, 407	419, 443	-	457	480
RM11-1a x S288C Δ*cgi121*	120, 121	139, 174	130, 146	240, 259	260, 303	296	358, 364	381, 407	419, 443	-	457	480
RM11-1a x S288C Δ*rps17a*	120, 121	139, 174	130, 146	240, 259	260, 303	296	358, 364	381, 407	419, 443	-	457	480
RM11-1a x S288C Δ*vma21*	120, 121	139, 174	130, 146	240, 259	260, 303	296	358, 364	381, 407	419, 443	-	457	480
RM11-1a Δ*cgi121* x S288C	120, 121	139, 174	130, 146	240, 259	260, 303	296	358, 364	381, 407	419, 443	-	457	480
RM11-1a Δ*rps17a* x S288C	120, 121	139, 174	130, 146	240, 259	260, 303	296	358, 364	381, 407	419, 443	-	457	480
RM11-1a Δ*vma21* x S288C	120, 121	139, 174	130, 146	240, 259	260, 303	296	358, 364	381, 407	419, 443	-	457	480

Figures

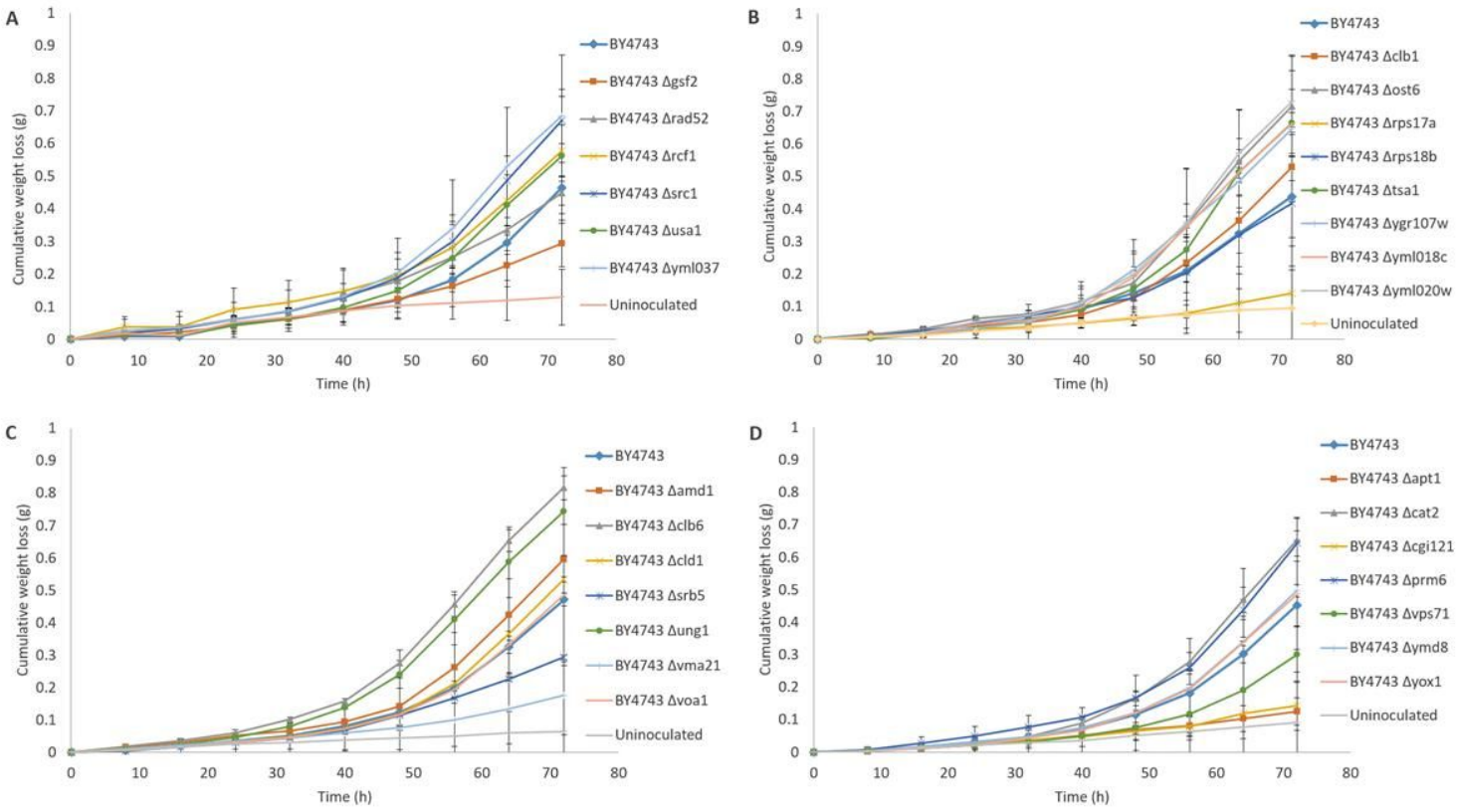

Figure 1

Average cumulative weight loss (g) of BY4743 and 28 BY4743 single gene deletion mutants fermented in synthetic grape medium at 15°C for 72 h (n = 3). A-D represent batches from 1-4 and each batch included BY4743 for standardization (series in bold). Error bars represent 95% confidence intervals.

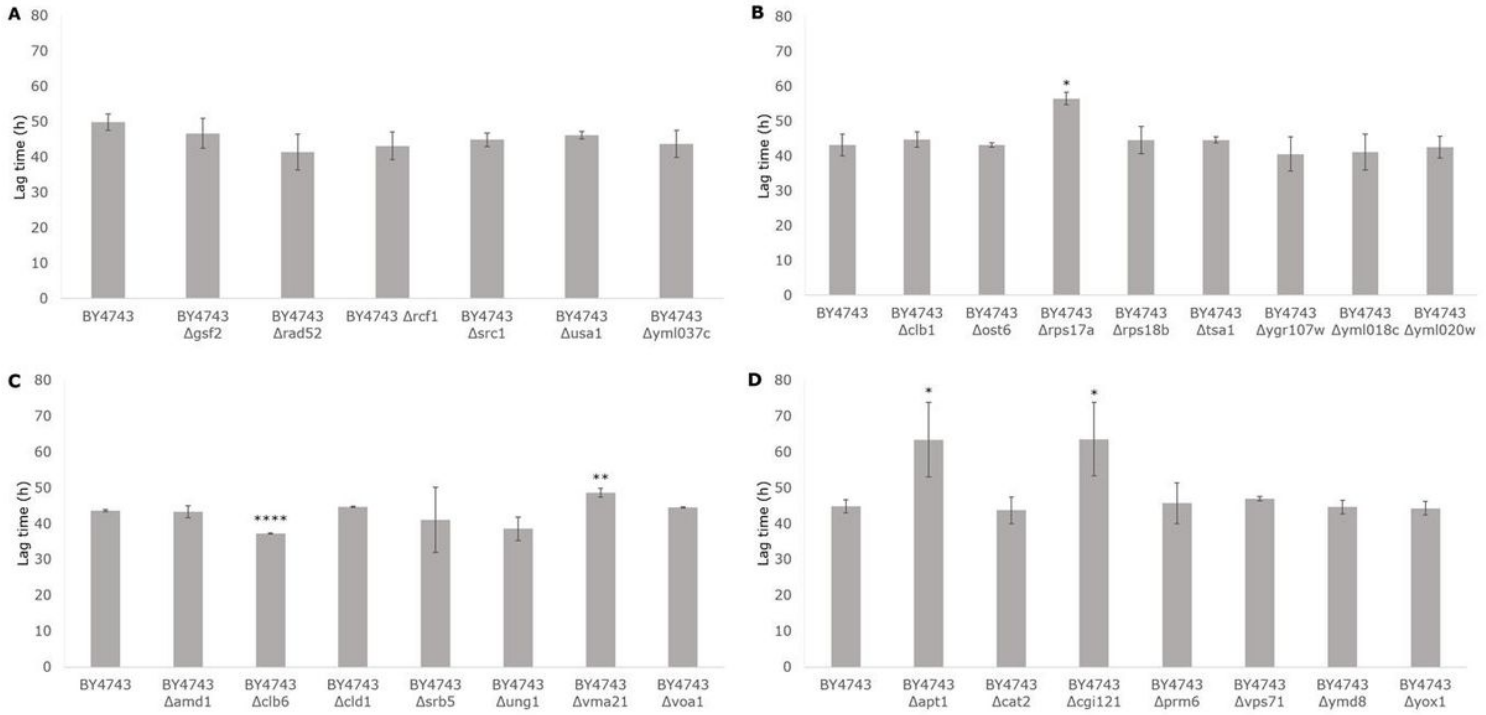

Figure 2

Lag time duration (h) of BY4743 and 28 BY4743 single gene deletion mutants fermented in synthetic grape medium at 15°C for 72 h (n = 3). A-D represent batches from 1-4 and each batch included BY4743 for standardization. Error bars represent 95% confidence intervals. Student's t-test was used to generate p-values between BY4743 and each single deletant ($p < 0.05$*, $p < 0.01$**, $p < 0.001$***, $p < 0.0001$****).

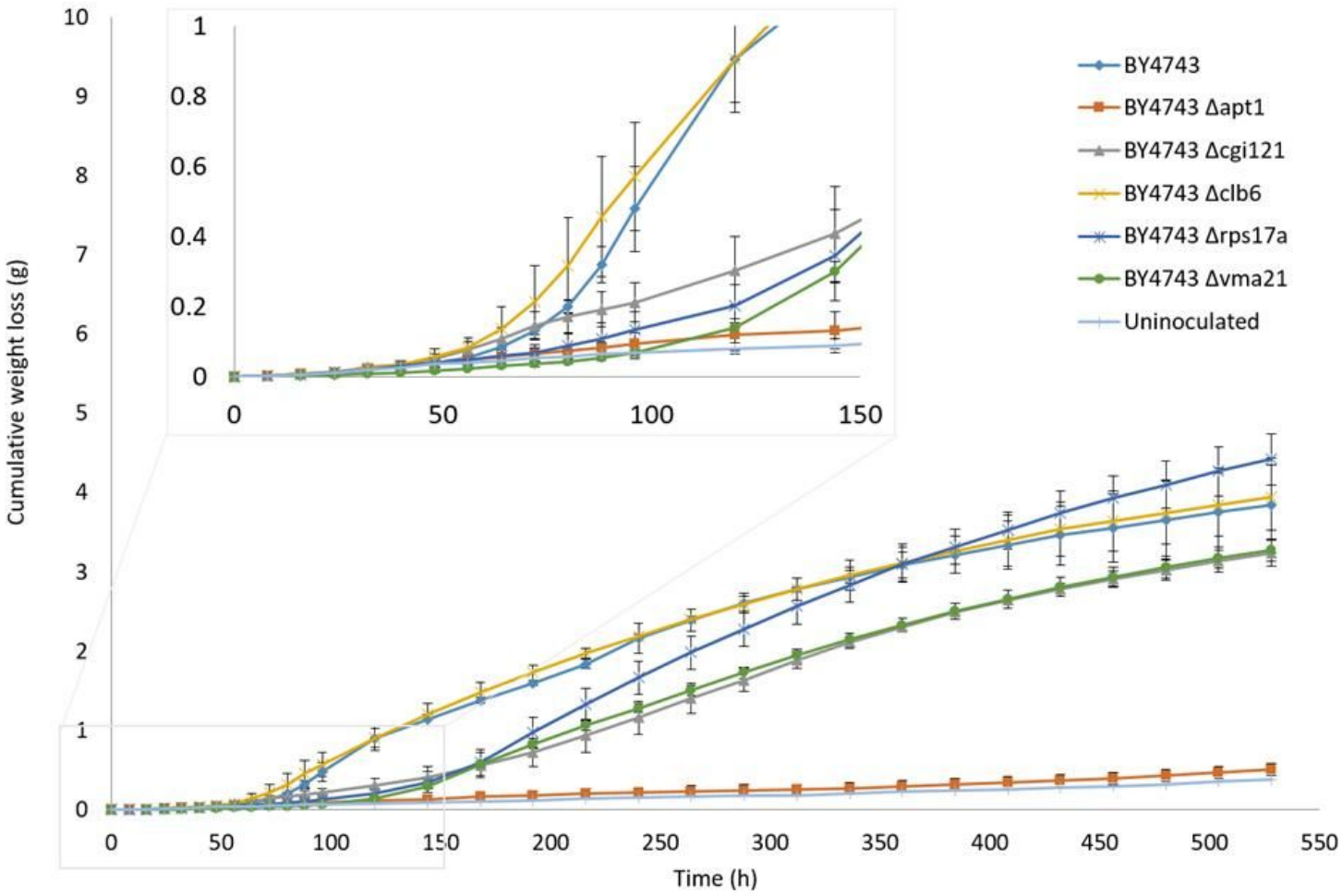

Figure 3

Average cumulative weight loss (g) of BY4743, BY4743 Δapt1, BY4743 Δcgi121, BY4743 Δclb6, BY4743 Δrps17a, and BY4743 Δvma21 fermented in synthetic grape medium at 12.5°C for 528 h (n = 3). A blow up of the graph is included to show the lag phase time more clearly. Error bars represent 95% confidence intervals.

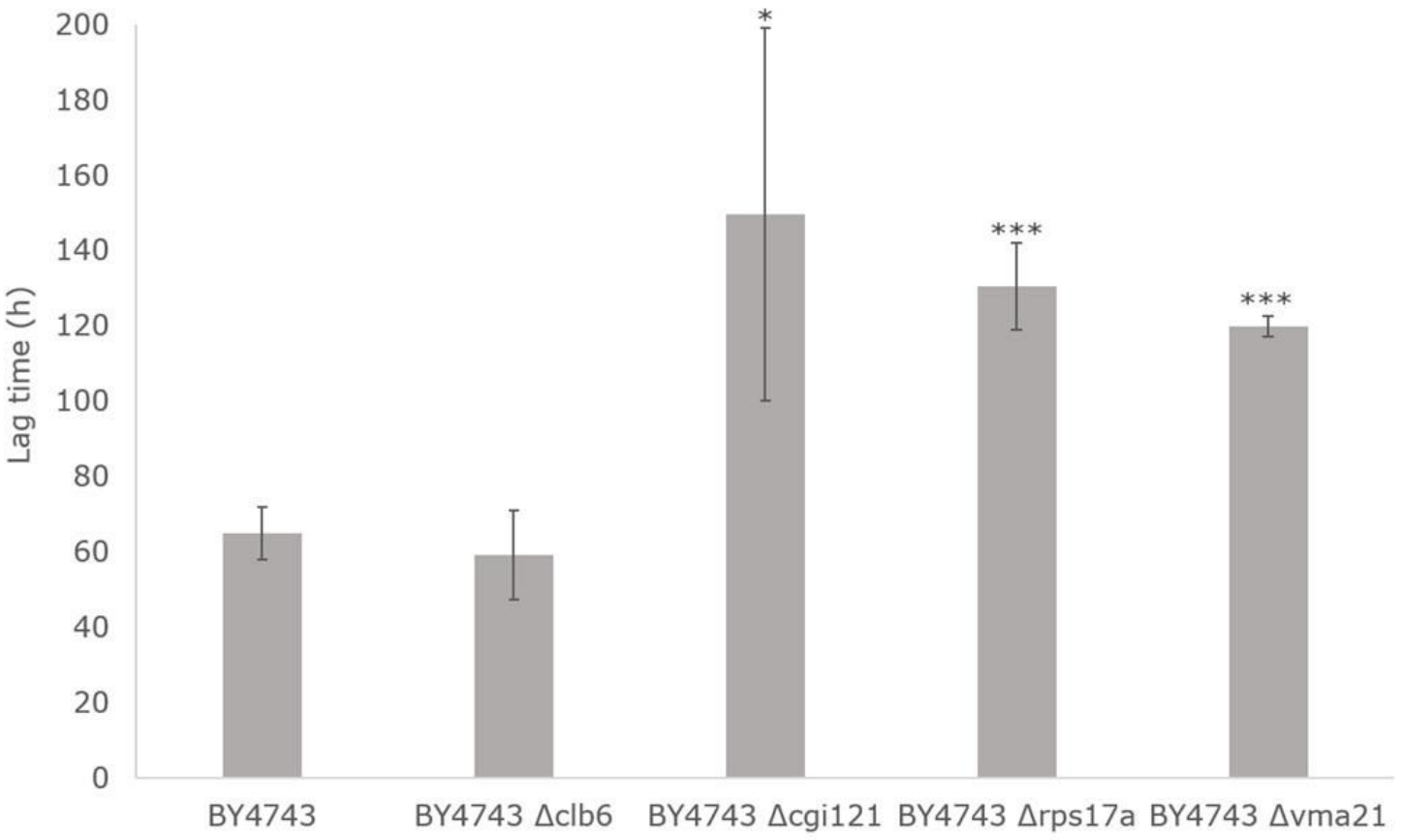

Figure 4

Lag time duration (h) of BY4743, BY4743 Δapt1, BY4743 Δcgi121, BY4743 Δclb6, BY4743 Δrps17a, and BY4743 Δvma21 fermented in synthetic grape medium at 12.5°C for 528 h (n = 3). Error bars represent 95% confidence intervals. Student's t-test was used to generate p-values between BY4743 and each single deletant ($p < 0.05$*, $p < 0.01$**, $p < 0.001$***).

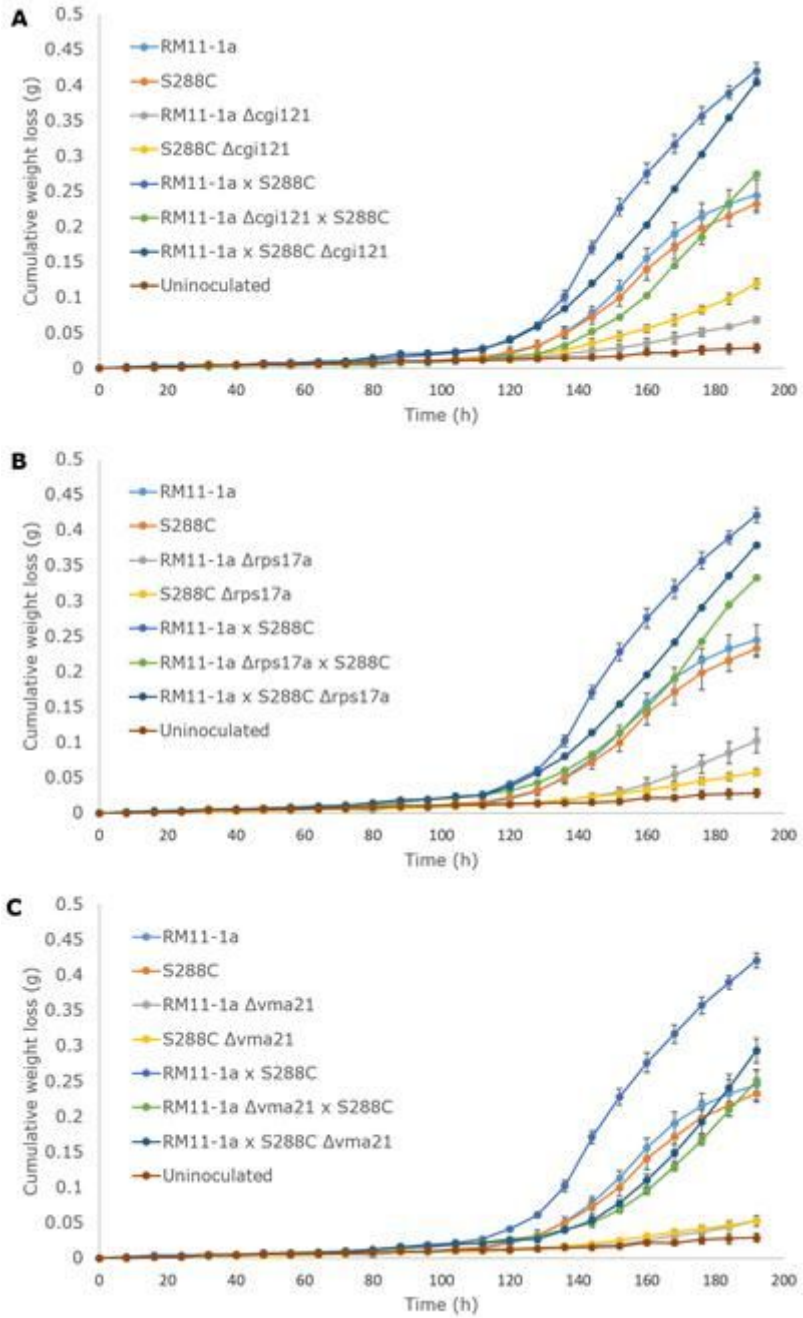

Figure 5

Average cumulative weight loss (g) of RM11-1a, S288C, and their corresponding single deletants and RHA hybrids for CGI121 (A), RPS17a (B), and VMA1 (C) fermented in synthetic grape medium at 12.5°C for 192 h (n = 3). Error bars represent 95% confidence intervals.

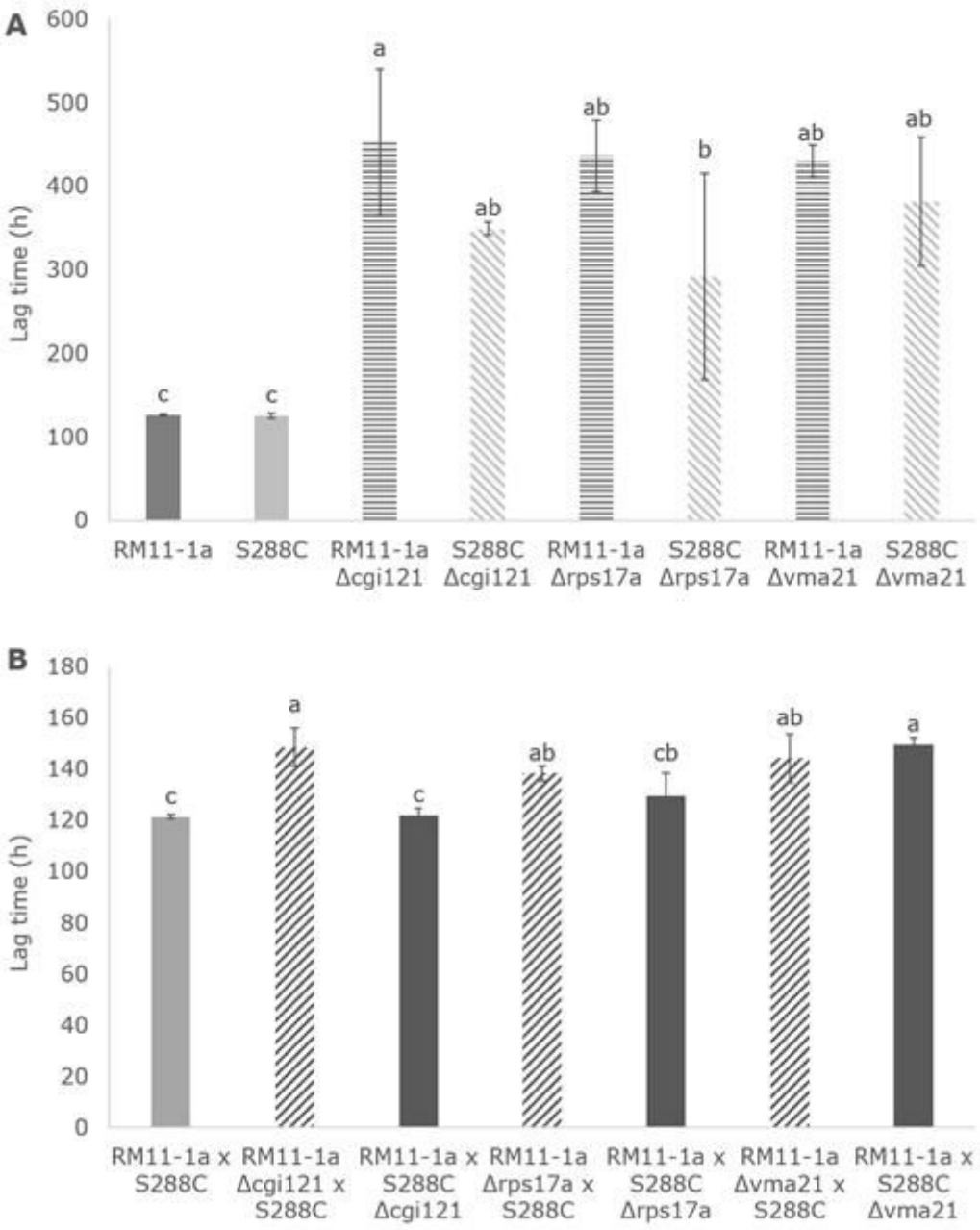

Figure 6

Lag time duration (h) of RM11-1a, S288C, and respective single deletants in Δcgi121, Δrps17a, and Δvma21 (A) and RHA hybrids comparing the impact of RM11-1a and S288C alleles of CGI121, RPS17a, and VMA1 (B) fermented in synthetic grape medium at 12.5°C for 192 h (n = 3). Error bars represent 95% confidence intervals. Samples sharing the same letter are not significantly different (ANOVA followed by post-hoc Tukey's HSD).

Supplementary Files

This is a list of supplementary files associated with this preprint. Click to download.

- LiDeedFileS1.docx